Physics Letters B 753 (2016) 204–210

Contents lists available at ScienceDirect

Physics Letters B

www.elsevier.com/locate/physletb

Exclusive measurements of quasi-free proton scattering reactions in inverse and complete kinematics

V. Panin [a,*], J.T. Taylor [b], S. Paschalis [a], F. Wamers [a,c], Y. Aksyutina [c], H. Alvarez-Pol [d], T. Aumann [a], C.A. Bertulani [e], K. Boretzky [c], C. Caesar [a], M. Chartier [b], L.V. Chulkov [f], D. Cortina-Gil [d], J. Enders [a], O. Ershova [g], H. Geissel [c], R. Gernhäuser [h], M. Heil [c], H.T. Johansson [i], B. Jonson [i], A. Kelić-Heil [c], C. Langer [g], T. Le Bleis [h], R. Lemmon [j], T. Nilsson [i], M. Petri [a], R. Plag [c], R. Reifarth [g], D. Rossi [c], H. Scheit [a], H. Simon [c], H. Weick [c], C. Wimmer [g]

[a] *Institut für Kernphysik, Technische Universität Darmstadt, 64289 Darmstadt, Germany*
[b] *Oliver Lodge Laboratory, University of Liverpool, Liverpool L69 7ZE, United Kingdom*
[c] *GSI Helmholtzzentrum für Schwerionenforschung, 64291 Darmstadt, Germany*
[d] *Departamento de Física de Partículas, Universidade de Santiago de Compostela, 15706 Santiago de Compostela, Spain*
[e] *Department of Physics and Astronomy, Texas A&M University-Commerce, Commerce, TX 75429, USA*
[f] *Kurchatov Institute, Ru-123182 Moscow, Russia*
[g] *Goethe-Universität Frankfurt am Main, 60438 Frankfurt am Main, Germany*
[h] *Physik Department E12, Technische Universität München, 85748 Garching, Germany*
[i] *Fundamental Fysik, Chalmers Tekniska Högskola, S-412 96 Göteborg, Sweden*
[j] *STFC Daresbury Laboratory, Daresbury, Warrington WA4 4AD, United Kingdom*

ARTICLE INFO

Article history:
Received 17 August 2015
Received in revised form 12 November 2015
Accepted 30 November 2015
Available online 10 December 2015
Editor: V. Metag

Keywords:
Quasi-free scattering
Inverse kinematics
Single-particle states
Spectroscopic factors

ABSTRACT

Quasi-free scattering reactions of the type $(p, 2p)$ were measured for the first time exclusively in complete and inverse kinematics, using a ^{12}C beam at an energy of ~400 MeV/u as a benchmark. This new technique has been developed to study the single-particle structure of exotic nuclei in experiments with radioactive-ion beams. The outgoing pair of protons and the fragments were measured simultaneously, enabling an unambiguous identification of the reaction channels and a redundant measurement of the kinematic observables. Both valence and deeply-bound nucleon orbits are probed, including those leading to unbound states of the daughter nucleus. Exclusive $(p, 2p)$ cross sections of 15.8(18) mb, 1.9(2) mb and 1.5(2) mb to the low-lying $0p$-hole states overlapping with the ground state $(3/2^-)$ and with the bound excited states of ^{11}B at 2.125 MeV $(1/2^-)$ and 5.02 MeV $(3/2^-)$, respectively, were determined via γ-ray spectroscopy. Particle-unstable deep-hole states, corresponding to proton removal from the $0s$-orbital, were studied via the invariant-mass technique. Cross sections and momentum distributions were extracted and compared to theoretical calculations employing the eikonal formalism. The obtained results are in a good agreement with this theory and with direct-kinematics experiments. The dependence of the proton–proton scattering kinematics on the internal momentum of the struck proton and on its separation energy was investigated for the first time in inverse kinematics employing a large-acceptance measurement.

Nuclear spectroscopy is one of the most fascinating areas of science, with applications in cosmology, stellar evolution, and even seemingly unrelated research areas such as material science. A strong confidence on the role of single-particle (SP) states in nuclear structure and nuclear spectroscopy arose with the work of Wigner, Mayer, and Jensen, recipients of the 1963 Nobel Prize, through the discovery and application of fundamental symmetry principles to nuclei and for realizing that much of the trend of nuclear masses and their energy spectra could be well understood by means of a simple SP shell model [1–3].

* Corresponding author at: RIKEN Nishina Center, RIBF Building 3F, 2-1 Hirosawa, Wako 351-0198, Japan. Tel.: +81 48 462 7946.
E-mail address: valerii.panin@riken.jp (V. Panin).

http://dx.doi.org/10.1016/j.physletb.2015.11.082

With the technical possibility of exploring nuclei far from the valley of β stability it was soon realized that the SP structure of nuclei is more of a local concept and it evolves with increasing proton–neutron asymmetry, at odds with the theoretical predictions. This shell evolution arises from terms in the nuclear interaction, which are not treated explicitly in the shell model, and which are enhanced only in neutron–proton asymmetric nuclei, placing their spectroscopy at the frontier of modern nuclear physics.

The large potential of studying the SP properties of nuclei by means of quasi-free nucleon–nucleon scattering (QFS) at high energy has been already realized by Chamberlain and Segrè [4] when they first observed this process pointing out the sensitivity to the intrinsic nucleon momentum distribution. Since then, QFS reactions of the type $(p, 2p)$ have been extensively used to study stable nuclei, see Refs. [5,6] for a review, and the work of Yosoi et al. [7] for a recent high-resolution measurement.

For the investigation of the shell structure of short-lived nuclei, nucleon-removal reactions have been employed in inverse kinematics using composite targets such as beryllium or carbon [8–10]. However, the sensitivity of such heavy-ion induced nucleon removal reactions is limited to the nuclear surface [11] and thus limits the accessible range of the bound-nucleon wave function, especially when a nucleon is removed from a deeply-bound shell in the case of exotic nuclei. In contrast to this, QFS reactions of $(p, 2p)$ and (p, pn) type are known to be sufficiently sensitive to both valence and deeply-bound shells [5,6,12].

In this Letter we present a new experimental approach to QFS reactions via inverse and complete kinematics measurements with a large-acceptance detection system. This technique results in minimum limitations on the observed kinematics (*e.g.*, scattering angles, energies, coplanarity, *etc.*) and provides complete information on the scattering process as well as on the structure of individual SP states. So far, proton-induced knockout reactions have been employed in inverse kinematics only in a more inclusive manner [13,14]. Furthermore, QFS in inverse kinematics is a very promising tool to investigate the role of nucleon–nucleon short-range correlations in neutron–proton asymmetric nuclei, including those induced by the tensor force, see Refs. [15,16] for two recent results from electron-induced knockout on stable nuclei. For such cases, the measurement in inverse kinematics offers the possibility to observe both the three outgoing nucleons as well as the beam-like heavy residue in coincidence.

Ideally, proton-induced QFS reaction is a sudden process with respect to internal motions of the nucleons in the nucleus in which a proton scatters elastically off a bound nucleon and both particles escape the nucleus without further interactions [5]. This creates a hole in the corresponding SP state, which can overlap with the ground state of the daughter nucleus or decay via γ-ray or particle emission, depending on the residual excitation energy E_x in the $(A-1)$ system and therefore on the separation energy $S_n = Q_n + E_x$ of the ejected nucleon, where Q_n is the nucleon separation threshold. Spectroscopic properties of the involved SP state, such as separation energy and internal momentum, can be extracted in two ways:

(i) by measuring the momenta of the recoil nucleons,
(ii) via direct measurement of the de-excitation of the $(A-1)$ system and its recoil momentum.

In direct-kinematics experiments, however, in which energetic protons irradiate stationary nuclear targets, the latter approach (ii) is very challenging. This is due to a relatively small momentum of the nuclear recoil, which prevents its escape from the target and complicates measurements of particle-unstable residual states. For this reason, detailed structure and fragmentation of deep-hole states are poorly known even in light stable nuclei [7]. In contrast, inverse kinematics in conjunction with full solid-angle coverage enables a redundant kinematical measurement of QFS reactions; this in turn allows a detailed study of correlations and final-state interactions to identify two-step processes.

The simplicity of the QFS reaction mechanism enables the use of the impulse approximation, which factorizes the reaction amplitude into a term associated with the elementary two-nucleon elastic scattering and a term corresponding to the nuclear part of the interaction alone [17]. However, there are two main sources of corrections entering the theoretical interpretation of experimental data. The first one is nuclear absorption, which can be taken into account by a complex optical potential which distorts the single-nucleon wave function [5,6,12]. The second one is purely technical and depends on the specific geometry of the experiment, *i.e.*, on angular and energy ranges of the measured nucleon pairs, which inevitably impose constraints on the observable energy and momentum space of the SP state as it is demonstrated in this Letter. In particular, most of the direct-kinematics QFS experiments so far have been performed in coplanar geometry, and only very few attempts were made to study experimentally and theoretically non-coplanar reactions [18–23]. Hence, large-acceptance experiments can become useful in extracting this information, although the absorption effects must still be taken into account carefully [22].

We are reporting on an experiment which was performed at the GSI Helmholzzentrum für Schwerionenforschung in Darmstadt, using the R^3B prototype setup [24], schematically shown in Fig. 1. A primary ^{12}C beam at an energy of 400 MeV/u was extracted from the heavy-ion synchrotron SIS18 and directed onto a 213(4) mg/cm^2 thick CH_2 target. The beam energy in the middle of the CH_2 target was ∼397.8 MeV/u. Complementary measurements with a 370(7) mg/cm^2 pure carbon target were carried out in order to extract the reaction contribution of the hydrogen component in the CH_2. Outgoing pairs of QFS protons were measured in the 4π-calorimeter Crystal Ball (CB), consisting of 159 NaI(Tl) crystals. Gamma-rays stemming from de-excitation of residual nuclei were also detected in the CB calorimeter. Additionally, the reaction chamber was equipped with an array of six AMS-type [25] 300 µm thick double-sided silicon-strip detectors (DSSDs) with a pitch of ∼100 µm. Four DSSDs downstream of the target aimed at the detection of QFS protons and covered the solid angle ranging from approximately 14° to 64° in the polar direction relative to the beam axis and to the geometrical center of the target. The two other DSSDs were placed on the beam axis at distances of 11 cm and 13.5 cm downstream of the target for charge identification and position measurements of kinematically forward-focused reaction fragments. The large dipole magnet ALADIN was situated at a distance of 1.5 m after the target and was used for separating heavy reaction products from breakup protons and neutrons. Each type of particle was separately measured after the magnet using time-of-flight Δt, energy-loss ΔE, and position information (x, y, z) in the corresponding tracking systems as shown in Fig. 1. Mass and charge resolutions below 3% were reached for the tracked $Z = 5$ fragments. Kinematically forward-focused neutrons from in-flight decay of excited fragments were detected around zero degree polar angle, using the Large Area Neutron Detector (LAND) [26] at a distance of around 14 m downstream of the target. Combining data from the different tracking arms allowed for the invariant-mass reconstruction of unbound $(A-1)$ fragments. Coarse angular information from two high-energy hits in the forward hemisphere of the CB was used to identify coincident proton hits in the DSSDs. Their outgoing angles were then reconstructed relative to the vertex in the target, which was obtained via backward tracking of the heavy fragment measured in the two in-beam DSSDs. Since the

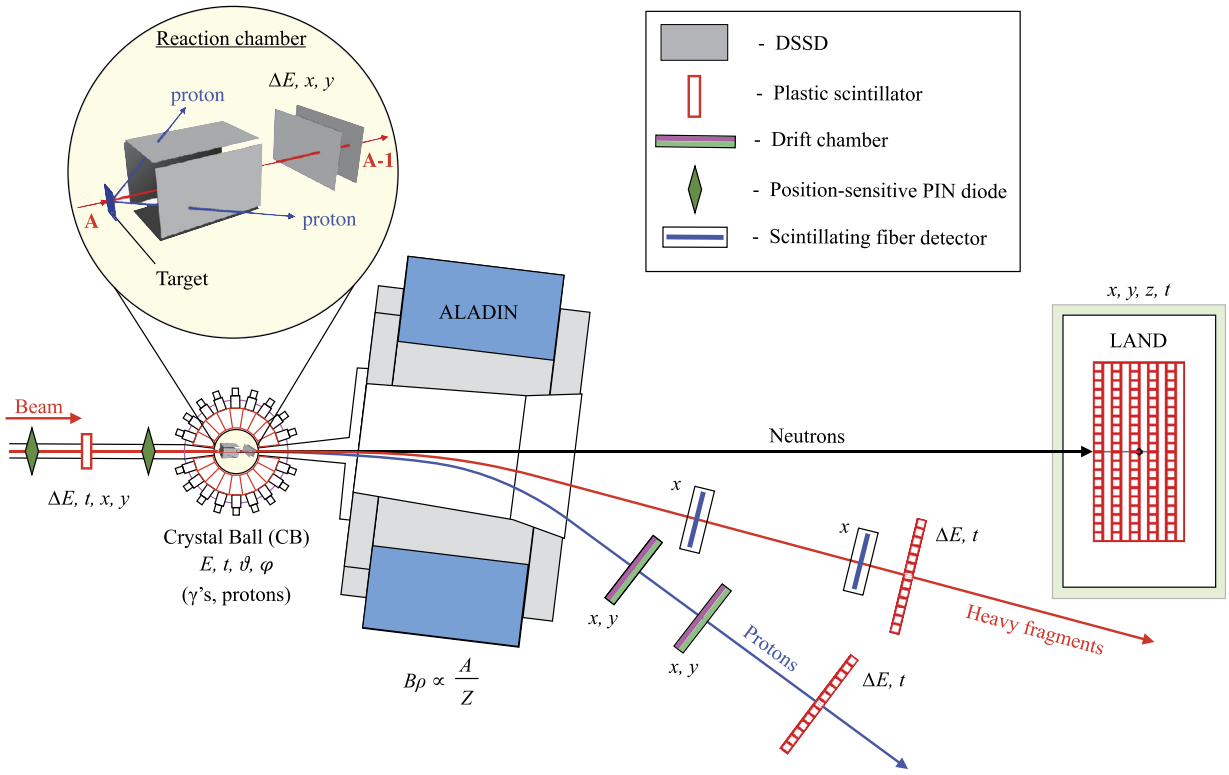

Fig. 1. Schematic layout of the experimental setup. The incident ^{12}C beam enters the setup from the left-hand side of the figure. The physical quantities measured with various detectors are indicated in the figure. The inset figure schematically shows a zoom of the arrangement of the target and DSSDs inside the reaction chamber. See text for more details.

high-energy protons were not fully stopped in the 20 cm long CB crystals, their energy measurements were not considered for the present analysis and only the trigger and angular data were taken into account.

The resulting two-proton angular correlations in coincidence with outgoing boron fragments are presented in Fig. 2, where carbon (C) and empty target (ET) data have been subtracted. The main background which has to be subtracted from the CH_2 data stems from carbon-induced reactions (around 20%), while empty target background amounts to less than 1%. The observation of a bound ^{11}B in the final state is interpreted as a proton knockout from the valence 0p-shell in ^{12}C. This corresponds to the separation energies $S_p < [Q_p(^{12}\mathrm{C}) + Q_\alpha(^{11}\mathrm{B})] = 24.621$ MeV, where $Q_p(^{12}\mathrm{C}) = 15.957$ MeV is the proton separation threshold in ^{12}C and $Q_\alpha(^{11}\mathrm{B}) = 8.664$ MeV is the lowest particle separation threshold in ^{11}B, *i.e.*, for ^{4}He. Fig. 2 displays a strong spatial correlation of outgoing protons, which is indicated by an opening angle (*i.e.*, the angle between the two protons as observed in the laboratory frame) around 80° and enhanced coplanar orientation of the scattering plane in azimuthal direction $|\Delta\varphi - 180°| \approx 0°$. The two lower frames of Fig. 2 show in addition the recoil-protons' angular distributions for the unbound final state $^{11}\mathrm{B}^* \rightarrow (^{10}\mathrm{B} + n)$, which can be interpreted as resulting from knockout from the inner 0s-shell. The peak of the opening-angle distribution is shifted to smaller values due to the larger separation energy $S_p > [Q_p(^{12}\mathrm{C}) + Q_n(^{11}\mathrm{B})] = 27.411$ MeV. It should be noted that the displacement and the width of the polar angle distribution, as compared to free p–p kinematics, corrected for the separation energy (solid black line in Fig. 2(a)), result from the separation energy on the one hand and from the magnitude and spatial orientation of the momentum of the knocked-out proton inside ^{12}C on the other hand. These two causes have similar effects on the outgoing angles and exceed by far the experimental angular resolution of approximately 1°. The coplanarity distributions for the 0p- and the 0s-state knockout are very similar due to competing effects; for this particular case: the $l = 0$ distribution (for a given separation energy) is narrower than for $l = 1$ (with the same separation energy). However, the much larger binding energy of the 0s-state makes the distribution wider, resulting in a rather similar width for the internal-momentum distributions (reflected by the width of the observed coplanar distribution) of the two cases. The measurement of the nucleon momentum distribution allows, in principle, to distinguish the l-value for a given separation energy [27,12].

Our results are in a good agreement with a kinematical simulation, which was adopted from another work [13].

The influence of the internal momentum on the angular distributions is also illustrated in the upper part of Fig. 3. As follows from the QFS reaction mechanism, the recoil momentum of ^{11}B in the rest frame of ^{12}C directly correlates with the internal momentum of the ejected proton. Combining the tracking information after the magnet with the angular measurements of the two in-beam DSSDs, the total, transverse, and longitudinal laboratory momenta of recoiling ^{11}B fragments were reconstructed event-wise. Their total momentum P_{tot} in the rest frame of ^{12}C was then calculated through the Lorentz transformation of their longitudinal part in the laboratory system. The resulting momentum resolutions (sigma) for the transverse and longitudinal part were estimated to be 20 MeV/c and 50 MeV/c, respectively. As apparent from the correlations shown in Fig. 3, non-coplanar events are related to larger internal momenta compared to coplanar events. In the lower frames of the same figure, the experimental momentum distributions are compared to theoretical calculations for 0p-shell proton knockout from ^{12}C [12], which make use of an eikonal theory with a quantitative description of the reaction mechanism, including absorption due to multiple-scattering effects and proper reaction

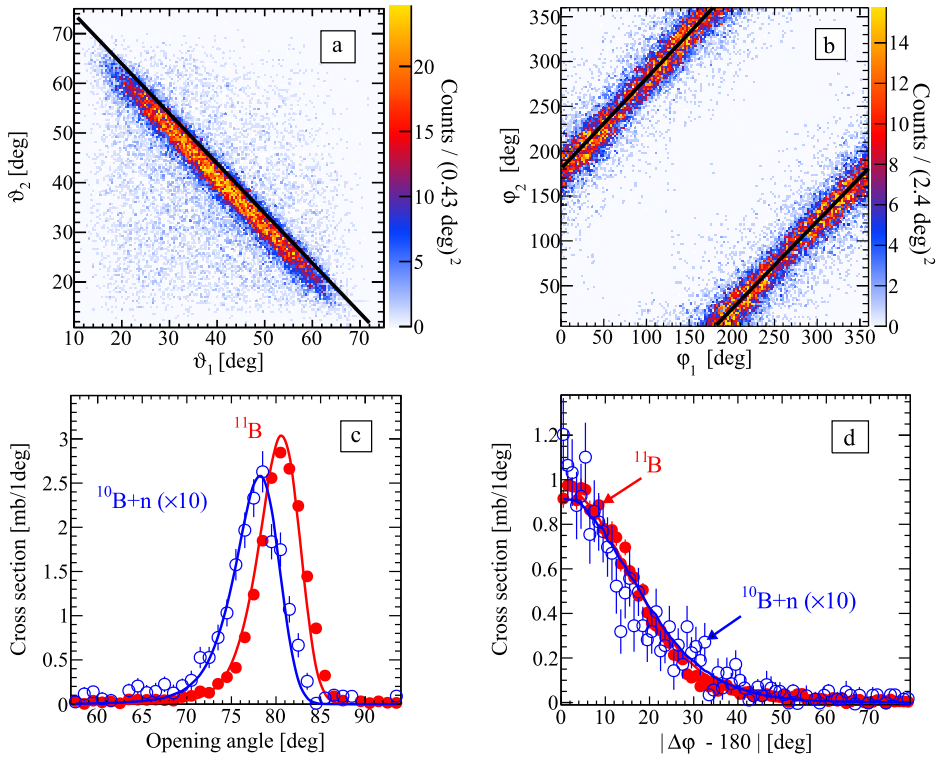

Fig. 2. Angular distributions of two outgoing protons observed for the hydrogen component of the target (CH_2 - C - ET) in coincidence with ^{11}B and $^{10}B+n$ in the final state. The coordinate system is defined relative to the direction of the incoming beam (polar axis). Correlations between polar (ϑ) and azimuthal (φ) angles in coincidence with outgoing ^{11}B are shown in frames (a) and (b), respectively, where the solid black lines indicate the result of the kinematical simulation, assuming 15.957 MeV separation energy and zero internal momentum for protons in ^{12}C. Frames (c) and (d) display angular distributions (see text for details) for ^{11}B (filled red circles) and $^{10}B+n$ (empty blue circles) in the final state, which are compared to kinematical simulations for each final state (red and blue solid lines, respectively). Only statistical errors are shown. The $^{10}B+n$ cross section data are scaled by the indicated factors for a better representation. (For interpretation of the references to color in this figure legend, the reader is referred to the web version of this article.)

kinematics. The model is similar to those adopted for knockout reactions with heavy ions [27] (more details can be found in Ref. [12]). The experimental data are in a good agreement with the theoretical calculations.

The total and partial cross sections measured for the $^{12}C(p, 2p)^{11}B$ reaction were efficiency corrected using the R3BRoot simulations [28] based on the FairRoot [29] platform, which included a complete description of the experimental setup. The adopted QFS kinematical code [13] has been used as an event generator for $(p, 2p)$ reactions, assuming isotropic center-of-mass proton–proton scattering. The CB response for the γ-rays, corresponding to the decay of the $0p$-hole excited states at 2.125 MeV $(1/2^-)$ and 5.02 MeV $(3/2^-)$ in ^{11}B, was determined through R3BRoot simulations, which included the simultaneous two-proton hits in the detector. An identical analysis procedure, as the one applied to the experimental data, was carried out with the simulated data. The simulated total two-proton detection efficiency in the CB was estimated to be around 62%. The variation of the two-proton efficiency due to the change in the kinematics for different final states and due to the presence of associated γ-rays was estimated to be less than 1%. The experimental γ-ray spectrum originating from the $^{12}C(p, 2p)^{11}B$ reaction was obtained through Doppler correction of the measured γ-ray energies in the CB. Carbon and empty target data were subtracted from the γ-spectrum measured with the CH_2 target in order to extract the H_2 contribution. Two-proton coincidence in the CB and an outgoing ^{11}B fragment were required in every case. The resulting spectrum contains two peaks, which can be attributed to the 2.125 MeV $(1/2^-)$ and 5.02 MeV $(3/2^-)$ excited states in ^{11}B. The experimental energy resolution for the full absorption peak is $\sigma_E/E \approx 10\%$ which is mainly due to given solid angles of individual CB crystals (≈77 msr/crystal). The final spectrum was fitted by the simulated response for each excited state and by the simulated background from two-proton hits in the CB, as shown in the inset in Fig. 4. Thus, partial cross sections of QFS knockout were determined for each excited state. The cross section to the ground state $(3/2^-)$ of ^{11}B was then calculated by subtracting the cross sections to the two excited final states from the total cross section of $19.2(18^{stat})(12^{sys})$ mb for the $^{12}C(p, 2p)^{11}B$ reaction. The results are summarized in Table 1 and compared to the theoretical $(p, 2p)$ SP cross sections, σ_{th}, calculated in the eikonal formalism [12]. The resulting spectroscopic factors, defined as the ratio of the experimental to theoretical SP cross sections, are given in the fourth column of Table 1 for each final state and are compared to those derived from other experiments including the $^{12}C(p, 2p)^{11}B$ measurement in direct kinematics [30], the results from $(e, e'p)$ [31], and the $(d, ^3He)$ [32] experiment with ^{12}C. Overall a very good agreement, not only for the relative, but also for the absolute spectroscopic factors, has been found. In total, around 65% of the expected $0p$ SP strength is found to be distributed among the three observed final states.

A detailed spectroscopic analysis of the deep-shell knockout cases, leading to unbound final states, is out of the scope of the present Letter and is only briefly discussed here to demonstrate the full potential of the proposed method. Due to the insufficient acceptance and limited multi-hit capabilities of the setup, only three two-body decay channels of ^{11}B were analyzed: $^{10}B + n$, $^9Be + ^2H$ and $^7Li + ^4He$, although a large number of events with three and more particles in the final state were also observed. Such many-body decays can be essential to understand the fragmentation mechanism of the $0s$-hole state in ^{11}B, as suggested by

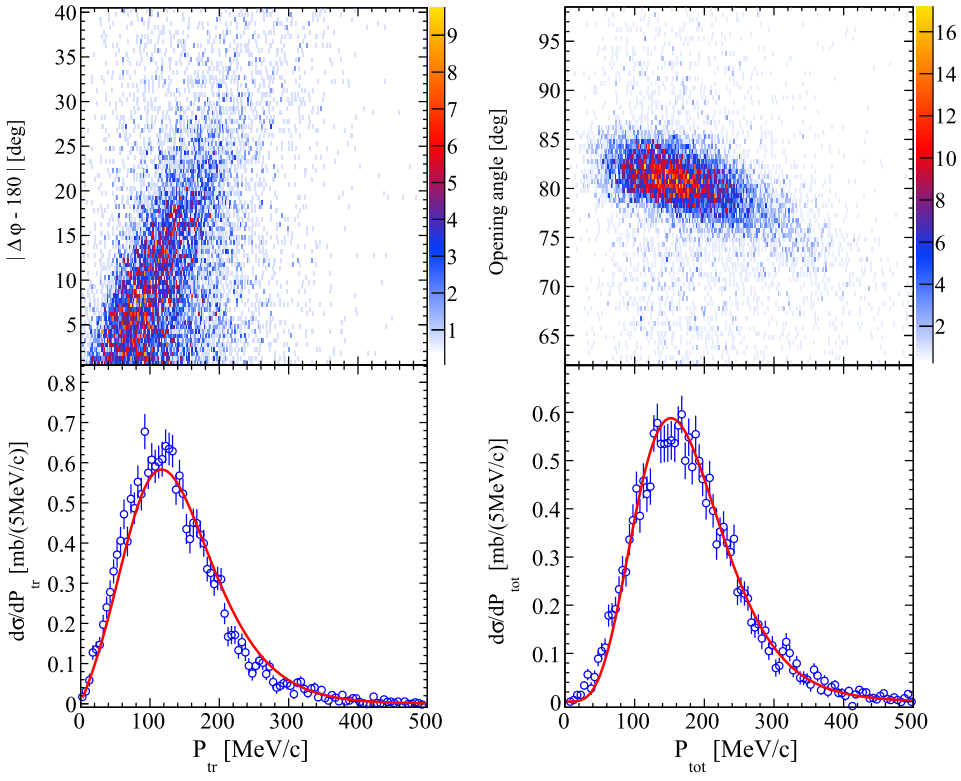

Fig. 3. Correlations of two-proton angular measurements in ^{12}C$(p,2p)^{11}$B reactions with transverse (left) and total (right) recoil momentum of ^{11}B in the rest frame of the incident ^{12}C. Bottom plots display the corresponding momentum distributions (circles) together with theoretical calculations (curves) for 0p-shell QFS knockout which take into account nuclear absorption effects (see text). The theoretical curves are normalized to the experimental data with the scaling factor of 0.64. As one can see, the coplanar angles correlate strongly with the transverse momentum, while the opening angle shows a dependence on the total internal momentum of the knocked-out proton as expected from the QFS kinematics due to energy conservation. All data are shown after subtraction of carbon and empty target contribution from the CH_2 data.

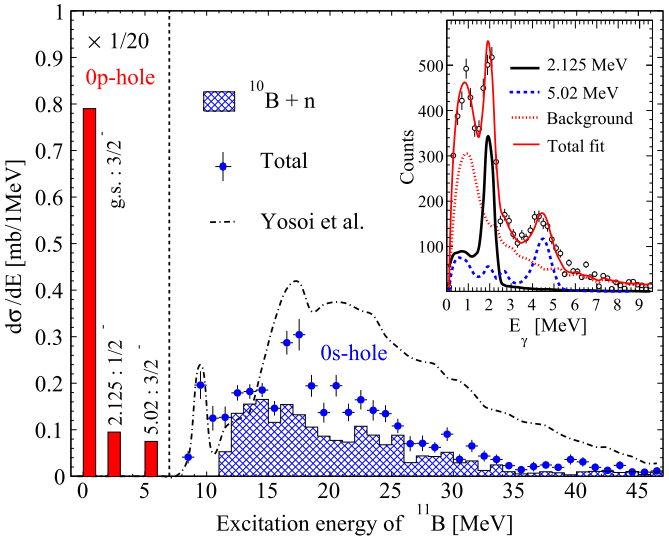

Fig. 4. Excitation spectrum of ^{11}B resulting from the ^{12}C$(p,2p)^{11}$B reaction. The left part of the spectrum (red filled bars) is reconstructed via γ-ray measurements (shown in the inset) of the excited bound states of ^{11}B as discussed in the text. The heights of the bars correspond to the integrated cross sections associated with the γ-decays (scaled down by a factor of 20). The right part of the spectrum (separated by the dashed line) shows the neutron breakup measurements (blue filled area) and the total reconstructed two-body breakup spectrum (blue filled circles). For a comparison the data from an inclusive $(p,2p)$ measurement [7] (dash-dotted line) is shown with an arbitrary scaling factor (see text). (For interpretation of the references to color in this figure legend, the reader is referred to the web version of this article.)

Yosoi et al. [7]. For instance, triton decay $^{11}\text{B} \rightarrow (^3\text{H} + ^4\text{He} + ^4\text{He})$ has a rather low threshold energy of 11.2 MeV and is expected to strongly compete or even to be a dominant process in the 2-body decay region and especially above 20 MeV. On the other hand, triton decay from the doorway ^{11}B (0s-hole) states is predicted to be significantly enhanced compared to statistical model calculations, thus reflecting the aspect of the 0s-hole spatial symmetry that follows from the microscopic cluster model [33].

The reconstruction of the neutron-breakup channel proceeded through simultaneous measurements of two-proton events in the CB, outgoing ^{10}B nuclei in the fragment arm, and single-neutron events in the LAND detector. The time-of-flight and position information from LAND was used to reconstruct the neutron velocity, momentum and angle. The relative angle between ^{10}B and the neutron was calculated event-by-event and the invariant mass of the initial ^{11}B was reconstructed. A simulation with the code LEG5 [34] has been performed in order to estimate acceptance and efficiency for single-neutron detection in LAND, which has been used to correct the reconstructed excitation-energy spectrum of the ^{11}B nucleus in the continuum. The result, after subtraction of the contribution from carbon-induced reactions and from empty-target run, is shown in Fig. 4 as the blue-hatched histogram. In a similar manner the excitation spectra from $^9\text{Be} + ^2\text{H}$ and $^7\text{Li} + ^4\text{He}$ decay channels have been reconstructed via the invariant-mass technique, utilizing the tracking information from the charged-particle detectors downstream of the target.

The resulting total excitation spectrum, comprising the above mentioned breakup channels, is shown in Fig. 4 as blue filled circles. In the same figure, the shape of the 0s-hole spectrum is compared to the data obtained in high-resolution $(p,2p)$ measure-

Table 1
Experimental QFS cross sections σ_{exp}, theoretical SP cross sections σ_{th} (see text for details) and corresponding spectroscopic factors S(exp) with their partial fractions relative to 1 (square brackets) for different final states in ^{11}B from ^{12}C$(p,2p)^{11}$B reactions. For a comparison, the spectroscopic factors from $(e,e'p)$ [31], $(p,2p)$ [30] and $(d,^3\mathrm{He})$ [32] experiments are shown.

E_x [MeV], J^π	σ_{exp}, mb	σ_{th}, mb [12]	S(exp)	$S(e,e'p)$ [31]	$S(p,2p)$ [30]	$S(d,^3\mathrm{He})$ [32]
0.0 (G.S.), $3/2^-$	15.8(18)	7.5	2.11(24) [0.82]	1.72(11) [0.79]	2.02 [0.76]	1.72 [0.82]
2.125, $1/2^-$	1.9(2)	7.4	0.26(3) [0.10]	0.26(2) [0.12]	0.33 [0.12]	0.27 [0.13]
5.02, $3/2^-$	1.5(2)	7.2	0.21(3) [0.08]	0.20(2) [0.09]	0.33 [0.12]	0.11 [0.5]
Total:	19.2(18)(12)[1]		2.58(30) [1.00]	2.18(15) [1.00]	2.68 [1.00]	2.1 [1.00]

[1] Statistical and systematical errors of the total cross section are given in the first and in the second parentheses, respectively. For other values in the table only total errors (if known) are shown inside parentheses.

ment [7], which was performed in direct coplanar kinematics with narrow angular and momentum acceptance. Since the comparison with our cross section, integrated over the full solid angle and momentum space is not straightforward, the data from Yosoi et al. was scaled by an arbitrary factor to match the peak around 10 MeV excitation energy. The two spectra show rather similar structures. The broad peak around 20 MeV can be associated with the proton knockout from the inner 0*s*-shell in ^{12}C. The lacking part of the cross section at higher excitation energies can be attributed to the many-body decay channels of ^{11}B nucleus, which have been omitted in the present analysis, such as $^{11}\mathrm{B} \rightarrow (^3\mathrm{H} + ^4\mathrm{He} + ^4\mathrm{He})$ discussed above.

In general, the intensity of the experiment is limited by the rate capability of the beam-tracking detectors, which are necessary for complete kinematical measurements with radioactive-ion beams, to about 10^5 particles per second. In the experiment reported here, the intensity was limited to 10^4 particles per second due to the time structure of the extracted beam from the synchrotron. However, the luminosity will be increased significantly in the future due to the use of a liquid hydrogen target. Also, the measurements of resolved gamma transitions from populated bound states limit the application to light nuclei with low level density. Nevertheless, in the future R^{3}B experiments bound and continuum states will be determined via missing-mass spectroscopy with the resolution of about 1 MeV or better due to more accurate momentum measurements of two outgoing protons.

In summary, we have presented a first-time exclusive measurement of $(p,2p)$ reactions in inverse and complete kinematics using as a benchmark case a ^{12}C beam at ∼400 MeV/u. Both the scattered protons as well as the heavy fragment and its decay products were measured and momentum analyzed. Angular correlations, momentum distributions, as well as excitation energy-spectra after one-proton knockout were extracted. The simultaneous measurement of scattered protons and heavy residues allowed for the first time to reveal the correlations between the angular distributions of the scattered protons and the intrinsic nucleon momentum carried by the recoil of the spectating $(A-1)$ fragment. Finally, spectroscopic factors for the 0*p*-states were derived by comparing to theoretical SP cross sections calculated through the eikonal formalism. The agreement between our results and the spectroscopic factors deduced from electron-induced knockout reactions demonstrates the validity of the proposed method, which we are confident will become a powerful tool for future studies with radioactive beams to investigate the SP structure of exotic nuclei.

Acknowledgements

The authors acknowledge support from HIC for FAIR, the GSI-TU Darmstadt cooperation agreement, the BMBF under Contract No. 05P12RDFN8, the Helmholtz Alliance EMMI, the Swedish Research Council, the U.S. NS Grant No. 1415656, the DOE grant No. DE-FG02-08ER41533 and the Spanish research agency CICYT under Project No. FPA2009-07387.

References

[1] M.G. Mayer, Phys. Rev. 75 (1949) 1969, http://dx.doi.org/10.1103/PhysRev.75.1969.
[2] O. Haxel, J.H. Jensen, H.E. Suess, Phys. Rev. 75 (1949) 1766, http://dx.doi.org/10.1103/PhysRev.75.1766.2.
[3] M.G. Mayer, Phys. Rev. 78 (1950) 16, http://dx.doi.org/10.1103/PhysRev.78.16.
[4] O. Chamberlain, E. Segrè, Phys. Rev. 87 (1952) 81, http://dx.doi.org/10.1103/PhysRev.87.81.
[5] G. Jacob, T.A. Maris, Rev. Mod. Phys. 38 (1966) 121, http://dx.doi.org/10.1103/RevModPhys.38.121.
[6] G. Jacob, T.A. Maris, Rev. Mod. Phys. 45 (1973) 6, http://dx.doi.org/10.1103/RevModPhys.45.6.
[7] M. Yosoi, et al., Phys. Lett. B 551 (2003) 255, http://dx.doi.org/10.1016/S0370-2693(02)03062-9.
[8] C.A. Bertulani, K.W. McVoy, Phys. Rev. C 46 (1992) 2638, http://dx.doi.org/10.1103/PhysRevC.46.2638.
[9] P.G. Hansen, J.A. Tostevin, Annu. Rev. Nucl. Part. Sci. 53 (2003) 219, http://dx.doi.org/10.1146/annurev.nucl.53.041002.110406.
[10] A. Gade, et al., Phys. Rev. C 77 (2008) 044306, http://dx.doi.org/10.1103/PhysRevC.77.044306.
[11] J. Hüfner, M.C. Nemes, Phys. Rev. C 23 (1981) 2538, http://dx.doi.org/10.1103/PhysRevC.23.2538.
[12] T. Aumann, C.A. Bertulani, J. Ryckebusch, Phys. Rev. C 88 (2013) 064610, http://dx.doi.org/10.1103/PhysRevC.88.064610, arXiv:1311.6734.
[13] L.V. Chulkov, et al., Nucl. Phys. A 759 (2005) 43, http://dx.doi.org/10.1016/j.nuclphysa.2005.05.148.
[14] T. Kobayashi, et al., Nucl. Phys. A 805 (2008) 431, http://dx.doi.org/10.1016/j.nuclphysa.2008.02.282.
[15] I. Korover, et al., Phys. Rev. Lett. 113 (2014) 022501, http://dx.doi.org/10.1103/PhysRevLett.113.022501.
[16] N. Fomin, et al., Phys. Rev. Lett. 108 (2012) 092502, http://dx.doi.org/10.1103/PhysRevLett.108.092502, arXiv:1107.3583.
[17] A.W. Stetz, Phys. Rev. C 21 (1980) 1979, http://dx.doi.org/10.1103/PhysRevC.21.1979.
[18] T. Yuasa, E. Hourany, Nucl. Phys. A 103 (1967) 577, http://dx.doi.org/10.1016/0375-9474(67)90924-4.
[19] E. Hourany, et al., Nucl. Phys. A 162 (1971) 624, http://dx.doi.org/10.1016/0375-9474(71)90260-0.
[20] T. Gooding, Nucl. Phys. 18 (1960) 46, http://dx.doi.org/10.1016/0029-5582(60)90384-9.
[21] Y. Sakamoto, Nucl. Phys. 46 (1963) 293, http://dx.doi.org/10.1016/0029-5582(63)90601-1.
[22] D.F. Jackson, Phys. Rev. 155 (1967) 1065, http://dx.doi.org/10.1103/PhysRev.155.1065.
[23] G. Jacob, T.A.J. Maris, Nucl. Phys. 20 (1960) 440, http://dx.doi.org/10.1016/0029-5582(60)90185-1.
[24] http://www.gsi.de/r3b, accessed: 2015-10-29.
[25] J. Alcaraz, et al., Nucl. Instrum. Methods Phys. Res., Sect. A, Accel. Spectrom. Detect. Assoc. Equip. 593 (2008) 376, http://dx.doi.org/10.1016/j.nima.2008.05.015.
[26] T. Blaich, et al., Nucl. Instrum. Methods Phys. Res., Sect. A, Accel. Spectrom. Detect. Assoc. Equip. 314 (1992) 136, http://dx.doi.org/10.1016/0168-9002(92)90507-Z.
[27] C.A. Bertulani, P.G. Hansen, Phys. Rev. C 70 (2004) 034609, http://dx.doi.org/10.1103/PhysRevC.70.034609.
[28] D. Bertini, J. Phys. Conf. Ser. 331 (2011) 032036, http://dx.doi.org/10.1088/1742-6596/331/3/032036.
[29] D. Bertini, M. A-Turany, I. Koenig, F. Uhlig, J. Phys. Conf. Ser. 119 (2008) 032011, http://dx.doi.org/10.1088/1742-6596/119/3/032011.
[30] D.W. Devins, et al., Aust. J. Phys. 32 (1979) 323.

[31] G. van der Steenhoven, et al., Nucl. Phys. A 480 (1988) 547, http://dx.doi.org/10.1016/0375-9474(88)90463-0.
[32] G.J. Kramer, H.P. Blok, L. Lapikás, Nucl. Phys. A 679 (2001) 267, http://dx.doi.org/10.1016/S0375-9474(00)00379-1, arXiv:nucl-ex/0007014.
[33] T. Yamada, M. Takahashi, K. Ikeda, Phys. Rev. C 53 (1996) 752, http://dx.doi.org/10.1103/PhysRevC.53.752.
[34] D.M. Rossi, et al., Phys. Rev. Lett. 111 (2013) 242503, http://dx.doi.org/10.1103/PhysRevLett.111.242503.